

A stochastic Lamb–Oseen vortex solution of the 2D Navier–Stokes equations

J. L. Sereno, J. M. C. Pereira and J. C. F. Pereira^{*,†}

*Instituto Superior Técnico, Mechanical Engineering Department, LASEF, Av. Rovisco Pais,
1049-001 Lisbon, Portugal*

SUMMARY

The exact solution of the Lamb–Oseen vortices is reported for a random viscosity characterized by a Gamma probability density function. This benchmark solution allowed to quantify the analytic error of the polynomial chaos (PC) expansion as a function of the number of stochastic modes considered and compare it with its numerical counterpart. The last was obtained in the framework of the PC expansion method together with a finite difference numerical discretization of the resulting system of Navier–Stokes equations for the expansion modes considered. The obtained solution may be used to test other numerical approaches for the solution of the Navier–Stokes equations with random inputs. Copyright © 2009 John Wiley & Sons, Ltd.

Received 13 May 2008; Revised 17 March 2009; Accepted 27 March 2009

KEY WORDS: vortex; Lamb–Oseen; stochastic; polynomial chaos; Navier–Stokes

1. INTRODUCTION

Vortex dynamics is a dominant phenomenon in many science fields and engineering applications. Among them and with aeronautical interest, the aircraft trailing vortices have received particular attention, see e.g. Pullin and Saffman [1], Gertz *et al.* [2]. For such real wake vortex and also for other systems, there are a great deal of uncertainty sources that may affect their formation and development.

Uncertainty quantification allows an insight into the scope of a physical system response providing an ensemble of solutions associated with a certain probability of occurrence. A method that has been recently applied for its effectiveness for short time integration for the calculation of stochastic partial differential equations (PDE's) is based on the spectral representation of random variables and has been called the polynomial chaos (PC) expansion method. Wiener [3] proposed a spectral representation of general random variables based on Hermite orthogonal polynomials of Gaussian random variables. The span of these orthogonal polynomials forms a complete basis for the L_2 space and has been called an PC. The PC representation of general random variables is convergent (in the L_2 sense) for the Gaussian measure, provided that the random variable is of second order, see Cameron and Martin [4]. This method was first applied in the context of PDE's in Ghanem and Spanos [5]. Later development of chaos decompositions based on non-Gaussian basic

^{*}Correspondence to: J. C. F. Pereira, Instituto Superior Técnico, Mechanical Engineering Department, LASEF, Av. Rovisco Pais, 1049-001 Lisbon, Portugal.

[†]E-mail: jcfpereira@ist.utl.pt

Contract/grant sponsor: EC; contract/grant number: AST4-CT-2005-012238
Contract/grant sponsor: FCT; contract/grant number: POCTI/EME/47012/2002

variables was made in Xiu and Karniadakis [6], which has been called the *Generalized Polynomial Chaos* and uses the orthogonal polynomials from the Askey family with weighting functions similar to probability density functions (Beta, Gamma, Binomial, etc.). A formal exposition and a generalization of the theory to arbitrary probability measures were accomplished in Soize and Ghanem [7]. Local PC expansions, suited for long-term integration and discontinuities in stochastic differential equations, were studied in Le Matre *et al.* [8] and in Wan and Karniadakis [9].

In this work we investigate the Lamb–Oseen vortices subjected to a random viscosity (Reynolds number) characterized by known PDF's. We present the analytic solution and compare the predicted PC expansion convergence error and the numerical approximation error.

The Lamb–Oseen vortices correspond to the exact solutions of the Navier–Stokes equations (see, e.g. Profilo *et al.* [10]) and have been extensively used as benchmark solutions for developing numerical methods and have initial or boundary conditions for various studies. Our interest is to predict their two-dimensional evolution subjected to a random viscosity (Reynolds number) and to investigate the interplay of the spacial discretization error with the stochastic approximation error. Furthermore, these solutions can be used to test new numerical methods designed for the stochastic Navier–Stokes equations.

2. STOCHASTIC NAVIER–STOKES EQUATIONS

A random variable (r.v.) can be represented using the PC expansion

$$X(\theta) = \sum_{n=0}^{\infty} a_n \Psi_n(\zeta(\theta)) \quad (1)$$

where the functions $\Psi_n(\zeta)$ are the orthogonal polynomials of the basic r.v. ζ defined in the inner-product space (L_w^2) with

$$\langle u, v \rangle = \int_{\Omega} uvw \, d\xi \quad (2)$$

w is the weighting function (defined in the domain Ω) and is often similar to certain probability density functions (Gaussian, Beta, Binomial, etc.). The θ parameter represents a random event and will be dropped to simplify the notation. Orthogonal polynomials that have weighting functions, which closely resemble PDF's can be found in the Askey family of hypergeometric polynomials [6]. A general differential equation containing random variables can be represented by

$$F(\mathbf{x}, t, \theta, \mathbf{u}) = f(\mathbf{x}, t, \theta) \quad (3)$$

where \mathbf{x} , t and θ represent the space coordinates, time and a random event. Substituting the expansion (1) in the differential equation we obtain the following equation:

$$F\left(\mathbf{x}, t, \theta, \sum_{n=0}^{\infty} \mathbf{u}_n \Psi_n\right) = f(\mathbf{x}, t, \theta)$$

The equation above must be projected into the space spanned by the polynomial basis defined earlier in order to absorb the random variable and to minimize the representation error. This procedure leads to

$$\left\langle F\left(\mathbf{x}, t, \sum_{n=0}^P \mathbf{u}_n \Psi_n\right), \Psi_k \right\rangle = \langle f(\mathbf{x}, t), \Psi_k \rangle$$

where the first $P+1$ terms were retained. This means that instead of solving a system of differential equations with random variables, one has to solve a larger system of coupled deterministic equations. The solution of Equation (3) is obtained usually by a sampling procedure, whereas the employed method leads to non-statistical method.

Assuming the PC expansion of the primary variables for the Navier–Stokes equations (for an incompressible fluid with constant properties)

$$\mathbf{u}(\mathbf{x}, t, \theta) = \sum_{n=0}^P \mathbf{u}_n(\mathbf{x}, t) \Psi_n(\zeta(\theta)) \quad (4)$$

$$p(\mathbf{x}, t, \theta) = \sum_{n=0}^P p_n(\mathbf{x}, t) \Psi_n(\zeta(\theta)) \quad (5)$$

and performing the projection into each element of the polynomial basis leads to the following system of deterministic PDE's:

$$\nabla \cdot \mathbf{u}_k = 0 \quad (6)$$

$$\frac{\partial \mathbf{u}_k}{\partial t} + \frac{1}{\|\Psi_k\|^2} \sum_{i=0}^P \sum_{j=0}^P e_{ijk} [\mathbf{u}_i \nabla] \cdot \mathbf{u}_j = -\frac{1}{\rho} \nabla p_k + \frac{1}{\|\Psi_k\|^2} \sum_{i=0}^P \sum_{j=0}^P e_{ijk} \nu_i \nabla^2 \mathbf{u}_j \quad (7)$$

where

$$e_{ijk} = \int_{\Omega} \Psi_i \Psi_j \Psi_k w(\xi) d\xi \quad (8)$$

and it was assumed that the viscosity is a r.v. The term e_{ijk} in Equation (7) is a sparse, constant and symmetric tensor and can be calculated *a priori*.

Equation (6) corresponds to the continuity equation and forms a set of independent differential equations, which means that all modes are divergence free. On the other hand, Equations (7) form a coupled set. These equations are coupled by the convective term and the diffusive term. An important aspect of these equations is that they are ‘equivalent’ for all the stochastic modes, which means that all modes are subjected to convection, diffusion and dissipation phenomena.

The solution of the system (6) and (7) provides the fields $\mathbf{u}_k(\mathbf{x}, t)$ and $p_k(\mathbf{x}, t)$, which may be used to calculate the approximate statistics (statistical moments, correlations and PDF's) of the flow.

The variance can be calculated using the expansion (1) and the orthogonality property of the polynomials. This is equal to the following inner product:

$$\begin{aligned} \langle u(x, t, \xi) - u_0(x, t), u(x, t, \xi) - u_0(x, t) \rangle &= \int_{\Omega} \sum_{i=1}^P u_i(x, t, \xi) \Psi_i(\xi) \sum_{j=1}^P u_j(x, t, \xi) \Psi_j(\xi) w(\xi) d\xi \\ &= \sum_{k=1}^P u_k^2(x, t) \|\Psi_k\|^2 \end{aligned} \quad (9)$$

where terms higher than P were neglected.

The Monte Carlo method is obtained by choosing the weighting function $w(\xi) = \delta(\theta - \theta_i)$, where δ is the Kronecker delta function and θ_i represents an outcome from a sampling procedure. A detailed description of the Monte Carlo methods can be found, e.g. in Hammersley and Handscomb [11].

3. NUMERICAL METHOD

The 4th order Runge–Kutta explicit time integration method together with sixth-order spatial central differences was used to solve the system of Navier–Stokes equations for the stochastic modes (see Equations (6) and (7)). The continuity equations (6) were used in a projection method to calculate each mode pressure field and to ensure that each velocity mode is divergence free. The Poisson equations for each mode were solved using the conjugate gradient method and the implicit Laplace operator was approximated recurring to a second-order scheme.

The computational cost of the numerical solution of the coupled set of equations is, with this method, approximately $(P+1)$ times higher than the cost of the numerical solution of the

corresponding deterministic problem because the Poisson equations for the pressure corrections are uncoupled.

The approximation error of this system has two origins, one is due to the truncation of series and the second is the numerical discretization. If ε_p^2 is the variance approximation error, then

$$\begin{aligned} \varepsilon_p^2 &= \left| \sum_{k=1}^{\infty} a_k^2(x, t) \|\Psi_k\|^2 - \sum_{k=1}^P \tilde{a}_k^2(x, t) \|\Psi_k\|^2 + \varepsilon_{\Delta x} \right| \\ &= \left| \underbrace{\sum_{k=1}^P (a_k^2(x, t) - \tilde{a}_k^2(x, t)) \|\Psi_k\|^2}_I + \underbrace{\sum_{k=P+1}^{\infty} a_k^2(x, t) \|\Psi_k\|^2}_II + \underbrace{\varepsilon_{\Delta x}}_{III} \right| \end{aligned} \tag{10}$$

In Equation (10) the approximation error sources correspond to: term *I* is the error due to the finite mode approximation where the computed modes $\tilde{a}_k(x, t)$ are different from the exact solution modes $a_k(x, t)$; term *II* is the error due to not considering stochastic modes higher than *P*; and term *III* is the numerical discretization error. These terms are not independent and it can occur that the magnitude of the terms higher than *P* is small, but the term *I* is large due to the coupling of the equations. These error sources will be referred as ε_I , ε_{II} and ε_{III} .

4. LAMB–OSEEN VORTICES UNDER A RANDOM VISCOSITY

The Lamb–Oseen vortex under a random viscosity characterized by a Gamma PDF was considered. This vortex is defined by the following equation in cylindrical polar coordinates:

$$v_{\theta} = \frac{\Gamma_c}{2\pi r} \left[1 - \exp\left(\frac{-r^2}{4vt}\right) \right] \tag{11}$$

where Γ_c is the circulation and r is the radius. A non-dimensional velocity, time and length will be used and an expected viscosity of $10^{-2} \text{ m}^2/\text{s}$ is considered so that a Reynolds number of approximately 100 was obtained. The reference velocity and time scale chosen are

$$(v_{\theta})_{\text{ref}} = \frac{\Gamma_c}{2\pi r_0} \tag{12}$$

$$t_{\text{ref}} = \frac{r_0}{(v_{\theta})_{\text{ref}}} = \frac{2\pi r_0^2}{\Gamma_c} \tag{13}$$

where r_0 was considered to be equal to 1. A random viscosity $v(\xi)$ was considered and from Equation (11) it is possible to conclude that for $r \rightarrow \infty$ the solutions will become increasingly closer to the potential flow solution, independently of the probability distribution considered. As could be expected, only the viscous vortex core is affected by the viscosity randomness.

Four different PDF's of the Gamma family were considered for the parameters $\alpha=0, 1, 2$ and 3 . For $\alpha=0$ the exponential PDF is recovered. The α parameter is related with the relative importance of events near $v=0$ and the parameter β influences the probability decay far from the mean value. The value of the β parameter was chosen so that the expected value of the viscosity corresponds to $v_0 = 10^{-2} \text{ m}^2/\text{s}$. The coefficient of variation (cv) for the Gamma PDF, considering an integer α , is given by

$$cv(\alpha) = \frac{1}{1+\alpha} \tag{14}$$

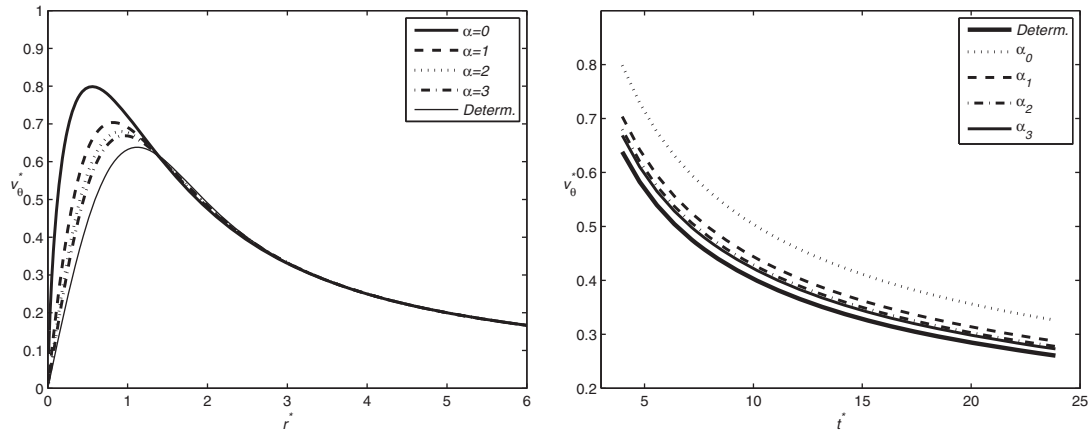


Figure 1. Stochastic solution for the *Gamma* viscosity. Left: mean velocity solutions for $t^* = \frac{25}{2}\pi$. Right: mean velocity decay.

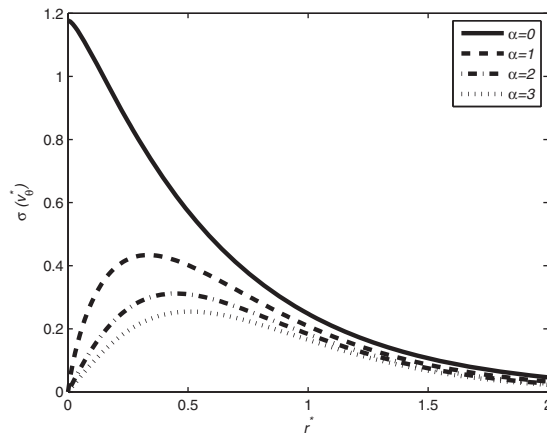


Figure 2. Variance of the stochastic solution for the *Gamma* viscosity for $t = \frac{25}{2}\pi$.

where the cv is the coefficient of variation, the quotient between the standard deviation and the mean value. The decrease of the α parameter will make the mean velocity solution depart from the deterministic solution (Figure 1 and Figure 3) due to the cv increase. It can be seen in these figures that the mean velocity solution varies considerably with the shape of the viscosity PDF. In average, the vortices will have a longer lifetime than predicted by the deterministic solution.

The variance is represented in Figure 2, where it can be seen that the uncertainty is restricted to the vortex core. For $\alpha = 0$ the variance peak is achieved at the vortex center, whereas in the other cases this maximum is achieved near the mean velocity peak inside the vortex core. The $\alpha = 0$ solution departs more from the deterministic case because in this case we have $cv = 100\%$.

The exact mean velocity solution for a general Gamma probability density function is given by the following equation:

$$E \left[\frac{v_{\theta}(r, \alpha, \beta, \zeta)}{(v_{\theta})_{\text{ref}}} \right] = \frac{r_0}{r} \left(\frac{2^{-\alpha} \left(\frac{r^2}{\beta t}\right)^{(1+\alpha)/2} J_{\alpha} \left(-1-\alpha, \frac{r}{\sqrt{\beta t}}\right)}{\Gamma(1+\alpha)} \right) \tag{15}$$

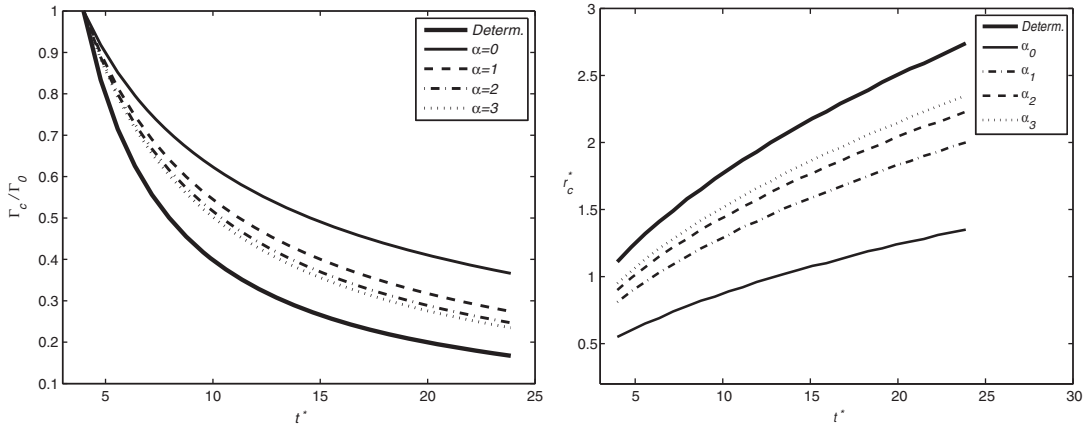


Figure 3. Stochastic solution for the *Gamma* viscosity. Left: vortex core circulation. Right: vortex core growth.

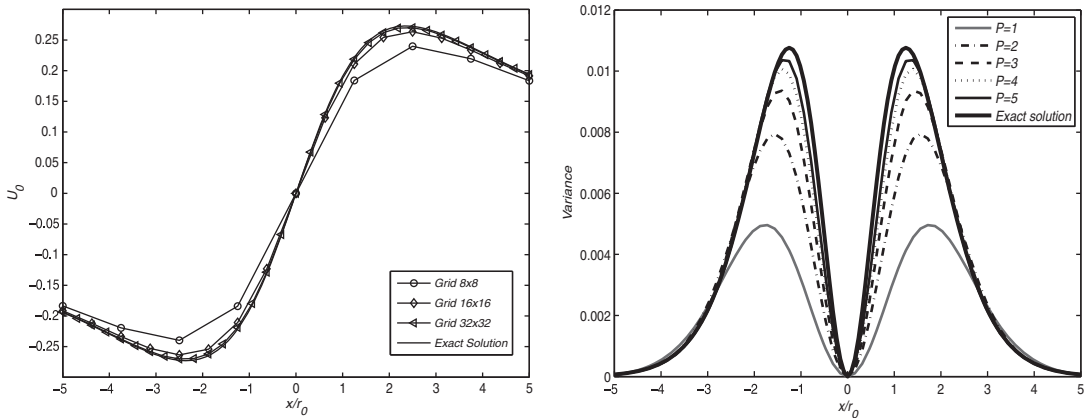


Figure 4. Stochastic numerical solution for a *Gamma* viscosity with $\alpha=3$. Left: mean velocity profile obtained with different spacial discretizations. Right: velocity variance obtained using a grid with 64×64 points.

and the non-centered velocity variance will be

$$\begin{aligned}
 E \left[\left(\frac{v_\theta(r, \alpha, \beta, \xi)}{(v_\theta)_{\text{ref}}} \right)^2 \right] &= \frac{2^{-\alpha}}{r^2 \Gamma(1+\alpha)} \left(2^\alpha \Gamma(1+\alpha) - 2 J_k \left(-1-\alpha, \frac{r}{\sqrt{\beta t}} \right) \left(\frac{r^2}{\beta t} \right)^{(1+\alpha)/2} \right. \\
 &\quad \left. + 2^{(1+\alpha)/2} J_k \left(-1-\alpha, \frac{\sqrt{2}r}{\sqrt{\beta t}} \right) \left(\frac{r^2}{\beta t} \right)^{(1+\alpha)/2} \right) \quad (16)
 \end{aligned}$$

where $\Gamma(x)$ is the Euler gamma function, an $J_k(v, x)$ is the modified Bessel function of the second kind.

4.1. Numerical results

The computational domain was chosen so that the viscous effects and its uncertainty were negligible at the boundaries location. Therefore, all PC expansion modes can be set to zero at the boundaries except the first ($P=0$), the mean solution is equal to the deterministic solution because the flow is irrotational in that region.

The mean velocity profile using several computational meshes and a PC expansion with $P=1$ is represented in Figure 4. Accurate results were obtained even for the minimal approximation level for the mean velocity solution, provided that a sufficient number of grid points were used. On the

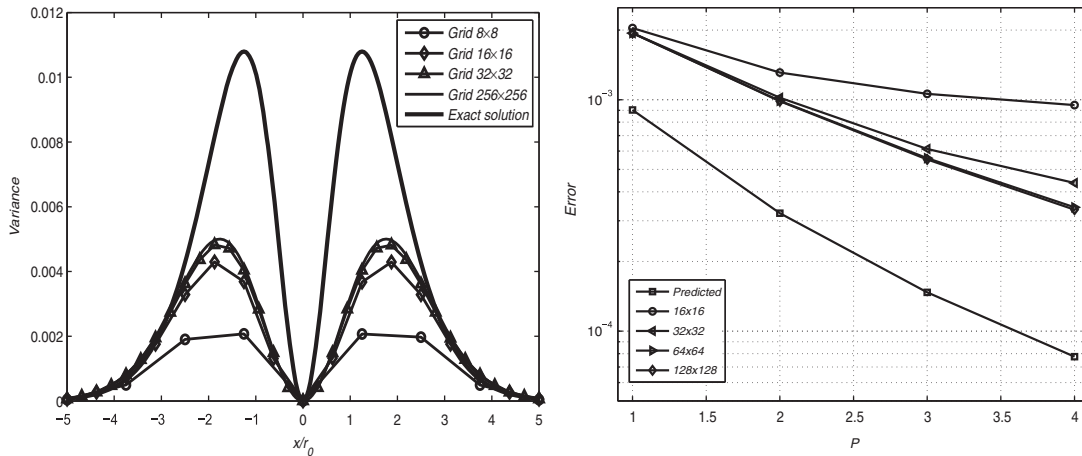


Figure 5. Left: comparison between different velocity variance computations. Right: numerical approximation $\|e\|_\infty$ error for the velocity variance.

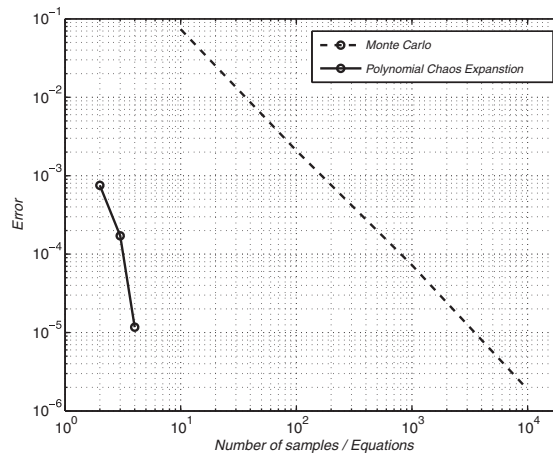


Figure 6. Comparison between the polynomial chaos expansion method and the Monte Carlo method.

other hand, a good approximation of the velocity variance was more difficult to obtain as can also be seen in Figure 4 where the results for PC expansions up to $P = 5$ are represented. The difference to the exact solution represented in this figure is related to the errors ε_{II} and ε_{III} described in Section 3. The variance approximation error components are clearly evidenced in Figure 5. The velocity variance computation can be improved by considering finer grids, but this is not sufficient because the overall numerical error reduction is also affected by the approximation level in the random variable. The exact solution for the U_1 expansion coefficient was calculated and is also represented in Figure 5. It can be seen that despite of the good numerical resolution considered the solution obtained with a *finite mode approximation* is far from the exact first mode U_1 solution. This large variance approximation error is related to the ε_{II} error source.

The predicted and numerical errors are represented in Figure 5. The numerical error obtained presented a similar behaviour to the predicted PC expansion error. Nevertheless, a saturation effect was found due to the stagnation of the convergence related to the interplay of the ε_I and ε_{II} with the numerical discretization error component ε_{III} . When coarse grids are used the ε_{III} error component becomes predominant causing the convergence rate to decrease. In Figure 6 the PC expansion method and the Monte Carlo method are compared using the assumption that the computational cost of the solution of the system of PDE's for the stochastic modes is proportional to the corresponding deterministic problem, as discussed in Section 2. The Monte Carlo solutions were obtained by sampling Equation (11) and the same, error of numerical variance, numerical

error measure was used. The PC expansion method was by far the most effective in capturing both the velocity mean and variance solution, being 10^3 faster than its counterpart.

For problems with low or moderate dimension very large improvements in the computational cost can be made relative to the cost of Monte Carlo. Adding a new equation (sample), when using the Monte Carlo method, has little influence on the statistics of the solution because the number of samples is usually large. If we consider the mean solution, for example, the effect of the new sample will be scaled by $1/N$, being N the overall number of samples. On the other hand, when using the PC method, an additional stochastic mode will make it possible to represent a larger set of stochastic processes. For example, in the case of the Gaussian PDF and Hermite polynomials, a two mode approximation can only represent fairly a symmetric PDF with similar tails to the Gaussian PDF. Adding another stochastic mode will make it possible to represent PDF's that are not symmetric, which corresponds to a qualitative improvement to the approximation of the random process.

4.2. Conclusions

The Lamb–Oseen vortex solution for the stochastic Navier–Stokes equations under a random viscosity field was presented and its approximation by the PC expansion method was studied. The analytic solutions were compared with several numerical approximations and the different error sources were described and quantified.

The results show that good approximations of the mean velocity solution can be obtained even when the minimal stochastic approximation with $P=1$ is considered if enough grid points are used. Accurate approximations for the velocity variance require additional stochastic modes, increasing the computational effort. The variance error was divided into three different dependent components: the ε_I which is related to the finite mode approximation with $P+1$ expansion terms, the ε_{II} error that accounts for the truncated terms of the PC expansion and the ε_{III} which is related to the numerical discretization error. If the grid is kept the same, increasing the number of PC expansion terms rapidly led to a saturation of the error decrease. In general, the effect of increasing the number of stochastic modes is more effective in reducing the approximation error than to double the number of grid points.

The set of solutions presented can be used as a benchmark for validation and error evaluation of stochastic Navier–Stokes equations solvers.

ACKNOWLEDGEMENTS

This work was partially supported by FAR-Wake project from the EC under Contract AST4-CT-2005-012238 and by FCT project POCTI/EME/47012/2002.

REFERENCES

1. Pullin DI, Saffman PG. Vortex dynamics in turbulence. *Annual Review of Fluid Mechanics* 1998; **30**:31–51.
2. Gerz T, Holzappel F, Darracq D. Commercial aircraft wake vortices. *Progress in Aerospace Sciences* 2002; **38**(3):181–208.
3. Wiener N. The homogeneous chaos. *American Journal of Mathematics* 1938; **60**:897–936.
4. Cameron R, Martin W. The orthogonal development of non-linear functionals in series of Fourier–Hermite functionals. *Annals of Mathematics* 1947; **48**(2):385–392.
5. Ghanem RG, Spanos P. *Stochastic Finite Elements: A Spectral Approach*. Springer: Berlin, 1991.
6. Xiu D, Karniadakis G. The Wiener–Askey polynomial chaos for stochastic differential equations. *SIAM Journal on Scientific Computing* 2002; **24**(2):619–644.
7. Soize C, Ghanem RG. Physical systems with random uncertainties: chaos representation with arbitrary probability measure. *SIAM Journal on Scientific Computing* 2004; **26**(2):395–410.
8. Le Matre OP, Najm HN, Ghanem RG, Knio OM. Multi-resolution analysis of Wiener-type uncertainty propagation schemes. *Journal of Computational Physics* 2004; **197**:502–531.
9. Wan X, Karniadakis G. An adaptive multi-element generalized polynomial chaos method for stochastic differential equations. *Journal of Computational Physics* 2005; **209**(2):617–642.
10. Profilo G, Soliani G, Tebaldi C. Some exact solutions of the two-dimensional Navier–Stokes equations. *International Journal of Engineering Science* 1998; **36**(4):459–471.
11. Hammersley JM, Handscomb DC. Monte Carlo Methods. *Methuen's Monographs on Applied Probability and Statistics*. Fletcher & Son Ltd: Norwich, 1964.